

## Magnetism in $\text{ErCo}_2$ under high pressure

O. Syshchenko,<sup>1,2</sup> T. Fujita,<sup>1</sup> V. Sechovský,<sup>2</sup> M. Diviš,<sup>2</sup> and H. Fujii<sup>3</sup>

<sup>1</sup>*Department of Quantum Matter, Hiroshima University, Higashi-Hiroshima 739-8526, Japan*

<sup>2</sup>*Department of Electronic Structures, Charles University, 121 16 Prague 2, The Czech Republic*

<sup>3</sup>*FIAS, Hiroshima University, Higashi-Hiroshima 739-8526, Japan*

(Received 29 June 2000; revised manuscript received 7 November 2000; published 12 January 2001)

We present results of experiments and *ab initio* calculations focused on the stability of Co magnetism in  $\text{ErCo}_2$  exerted to high pressures. In the experiments we have studied pressure effects on electrical-resistivity anomalies in the vicinity of Curie temperature ( $T_C = 33$  K in ambient pressure) that are intimately related to the formation and ordering of Co itinerant  $3d$  electron moments. The Co magnetism in this material is a consequence of the itinerant electron metamagnetism (IEM) induced in a large exchange field appearing at  $T_C$  where the localized Er moments order ferromagnetically. At lower pressures,  $T_C$  decreases linearly with increasing pressure  $p$  ( $\partial \ln T_C / \partial p = 0.24 \text{ GPa}^{-1}$ ). Magnetovolume measurements under pressure and magnetic-moment calculations performed for reduced lattice parameters reveal that also the Co moment decreases with increasing pressure. At higher pressures, the  $T_C$  vs  $p$  dependence strongly deviates from the initial linear trend and above a critical pressure  $p_c \approx 4$  GPa, the  $T_C$  becomes nearly pressure independent. To explain this behavior we propose a scenario assuming that for  $p > p_c$  the  $3d$  band broadens to such extent that the projected Co- $3d$  density of states in the vicinity of  $E_F$  decreases critically and the Er-Co-Er exchange channel becomes ineffective to induce the IEM. The Er sublattice then orders at much lower temperature  $T_C \approx 13$  K, which is determined by the Er-Er interaction channel mediated by conduction electrons. This scenario is corroborated by results of the *ab initio* calculations that indicate the collapse of IEM in pressures above a certain value.

DOI: 10.1103/PhysRevB.63.054433

PACS number(s): 75.30.Kz

### I. INTRODUCTION

The Co  $3d$ -band states in the  $R\text{Co}_2$  ( $R$ : rare-earth element) compounds appear near the critical conditions for Co-moment formation. The Co  $3d$  moment instability makes the  $R\text{Co}_2$  compounds frequent objects of intensive experimental and theoretical studies of various aspects of the itinerant electron magnetism.<sup>1,2</sup> The compounds with the nonmagnetic  $R$  elements,  $\text{YCo}_2$  and  $\text{LuCo}_2$ , are exchange-enhanced paramagnets. At sufficiently low temperatures they exhibit a metamagnetic transition (MT) with a critical field  $\mu_0 H_c \approx 70$  T.<sup>1</sup> The high-field state in  $\text{YCo}_2$  and  $\text{LuCo}_2$  characterized by a ferromagnetic ordering of Co  $3d$  moments is a consequence of a sudden splitting of the majority- and minority-spin  $3d$  subbands at  $H_c$ . This phenomenon called itinerant electron metamagnetism (IEM) is closely related to the instability of itinerant electron ferromagnetism. It can be explained in terms of Landau theory of phase transitions that allows us, as proposed by Wohlfarth and Rhodes,<sup>3</sup> to define the necessary conditions for the appearance of IEM.

$\text{YCo}_2$  and  $\text{LuCo}_2$  are frequently quoted as the archetypes of spin-fluctuation systems with a high characteristic temperature  $T_{\text{sf}}$ , which correlates with the temperature of susceptibility maximum  $T_{\text{max}}$ . Considering the role of spin fluctuations, Yamada has formulated a theory of IEM accounting for the finite-temperature behavior.<sup>4</sup>

The lattice volume of  $R\text{Co}_2$  compounds is the principal parameter intimately connected with the  $3d$ -band width. The role of lattice volume in the appearance of IEM has been demonstrated by the recent total-energy fixed-spin-moment calculations performed for  $\text{YCo}_2$  with values of the lattice parameter taken from all the members of the  $R\text{Co}_2$  series.

Results of these calculations indicate that IEM occurs between  $\text{TbCo}_2$  and  $\text{DyCo}_2$ ,<sup>5</sup> which is in agreement with experiment. Note that the lattice volume of  $\text{YCo}_2$  is near to that of  $\text{HoCo}_2$  and due to the lanthanide contraction,  $\text{LuCo}_2$  is characterized by even smaller lattice.

The IEM in  $\text{ErCo}_2$  and some other heavy  $R$  counterparts ( $\text{DyCo}_2$  and  $\text{HoCo}_2$ ) is, however, observed in zero external magnetic field. In these materials, the Co metamagnetic state is induced in a large effective exchange field, which is mediated from the ferromagnetically ordered  $R$   $4f$  moments by the  $5d(R)$ - $3d(\text{Co})$  hybridization. This field emerges at  $T_C$  ( $=33$  K for  $\text{ErCo}_2$ ) when the  $R$  sublattice orders ferromagnetically.<sup>6</sup> Consequently, a first-order magnetic phase transition (FOMPT) accompanied by a dramatic drop of the electrical resistivity and a sudden volume expansion is observed at  $T_C$ . These phenomena reflect the abrupt change of the density of Co  $3d$  states at  $E_F$  and a partial localization of the  $3d$  states as a consequence of the splitting of the majority and minority spin sub-bands and the associated Co moment formation.

The existence of  $3d$  electron metamagnetism in  $\text{ErCo}_2$ -type compounds has been confirmed by numerous experiments.<sup>7-10</sup> It has been shown that the value of the Co moment  $\mu_{\text{Co}} \approx 1 \mu_B$  when the effective field  $H_{\text{eff}}$  acting on  $3d$  electrons is higher than a critical value  $H_c$  ( $\sim 100$  T), but it becomes dramatically reduced as soon as  $H_{\text{eff}} < H_c$ . When diluting the magnetic  $R$  atoms by nonmagnetic Y atoms,  $T_C$  decreases and the related FOMPT is replaced by the second-order magnetic phase transition (SOMPT) for a sufficiently high Y content. This happens for a certain critical concentration of Y that yields reduction of the  $H_{\text{eff}}$  value as much as  $H_{\text{eff}} < H_c$ . For the critical concentration region a sharp peak-

like  $\rho(T)$  anomaly develops just above  $T_C$ .<sup>2,11</sup> Bloch *et al.* have suggested that the FOMPT in  $\text{ErCo}_2$  can be changed to the SOMPT also by applying high pressure.<sup>12</sup>

In his theoretical work,<sup>13</sup> Yamada has considered the effect of pressure on the itinerant  $3d$  electron subsystem at finite temperatures. The effect of spin fluctuations has been taken into account in the phenomenological Landau-Ginzburg theory. He has concluded that  $H_c$  increases with increasing pressure and the MT vanishes at a critical pressure  $p_c$ . The  $p_c$  value decreases with increasing temperature and becomes zero at a critical temperature  $T_0$ . Values between 1 and 5 GPa have been estimated for  $p_c$  in  $\text{YCo}_2$  at 0 K.

In order to see effects of variation of interatomic distances on magnetism in  $\text{ErCo}_2$  in detail, we study in this work pressure effects on the resistivity anomalies in the vicinity of  $T_C$ . Simultaneously, we have performed *ab initio* electronic structure calculations based on density functional theory (DFT) on  $\text{ErCo}_2$  for the ambient-pressure lattice parameter  $a$  and also for several reduced  $a$  values expected for some applied pressures. A similar pressure experiment with  $\text{ErCo}_2$  was performed by Hauser *et al.*<sup>14</sup> in pressures up to 6 GPa using a Bridgman cell (above 1.5 GPa).

## II. DETAILS OF EXPERIMENT AND FIRST-PRINCIPLES CALCULATIONS

The polycrystalline  $\text{ErCo}_2$  sample was synthesized by arc melting the components (minimum purity of 3N5) under argon atmosphere. An Er:Co ratio of 1:1.95 has been chosen to avoid formation the ferromagnetic  $\text{ErCo}_3$ . The melted button was then annealed at 650 °C in vacuum for 14 days. The x-ray-diffraction analysis revealed only the expected cubic C15 phase with a lattice constant that is in a good agreement with literature data. The electrical resistivity was measured as a function of temperature ( $4.5 < T < 300$  K) on a bar-shaped sample (size  $\sim 0.2 \times 0.2 \times 0.8$  mm<sup>3</sup>) using the dc four-terminal measuring technique. The values of  $T_C$  were associated with the temperature of maximum  $\partial\rho/\partial T$ . The pressure experiment was performed by using a cubic-anvil device<sup>15</sup> with a mixture of Fluorinert FC 70 and FC 77 as a pressure-transmitting medium. The sample was put into a cylindrical Teflon cell with an inner space of 1.5 mm diameter and 1.5 mm length and current was applied parallel the axis of cylinder. Vitrification of the fluid medium at low  $T$  often causes a slight deviation from hydrostaticity, though the applied pressure is completely hydrostatic when the pressure medium remains fluid. Pressure applied to the anvil unit was held constant within 3% during the temperature sweeps. In this system a quasihydrostatic pressure can be generated by isotropic movement of six anvil tops even after the fluid medium vitrifies at low temperature and high pressure. The key feature of our measurement is that, in our cubic anvil device, the hydrostaticity strongly depends on the sample shape and size because of a difference in the compressibility between the sample and the vitrified mixture. It was found<sup>16</sup> that for the bar-shaped sample with dimensions  $0.23 \times 0.25 \times 0.73$  mm<sup>3</sup> which is close to the size of our sample the anisotropic pressure ratio  $p_{\parallel i}/p_{\perp i}$  is about 1.1 where  $p_{\parallel i}$  and  $p_{\perp i}$  denote the pressure applied along and perpendicular to

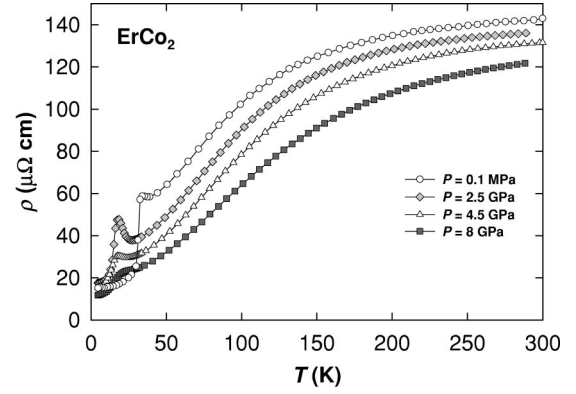


FIG. 1. Temperature dependence of electrical resistivity of  $\text{ErCo}_2$  at various pressures.

the longest dimension of the sample. In our measurement the pressure up to 8 GPa has been applied.

To obtain relevant information on electronic structure of  $\text{ErCo}_2$ , first-principles theoretical calculations based on the density-functional theory (DFT) were performed. Exchange and correlation effects are treated within the local spin-density approximation (LSDA) and the general gradient approximation (GGA).<sup>17</sup> The scalar relativistic Kohn-Sham equations were used to obtain the self-consistent single-electron wave functions. The calculations were performed using the full potential linearized augmented plane-wave method (LAPW) implemented in the latest version (WIEN97) of the original WIEN code.<sup>18</sup> Atomic sphere (AS) radii of 2.8 and 2.3 a.u. were taken for Er and Co, respectively. The basis functions were represented by approximately 850 plane waves (more than 120 APW/atom) plus local orbitals of Er ( $5s, 5p$ ) and Co ( $3p$ ) semicore states, which lie less than 6 Ry below the Fermi level. A maximum of  $l_{\text{max}} = 12$  was adopted for the expansion of the radial wave function. Inside the spheres the crystal potential and charge density were expanded into crystal harmonics up to the 6th order. For the Brillouin zone (BZ) integration a tetrahedron method<sup>18</sup> with 72–286  $k$  points was used in the irreducible wedge corresponding to the 2000–10 000  $k$  points in the full BZ. We carefully checked that the above described computational details provide highly converged DFT results for the compound studied.

To simulate the localized  $4f$  states, the hybridization of the  $4f$  states with all other valence states was switched off and the Er  $4f$  states were treated in the spherical part of the crystal potential as atomiclike core states (open-core treatment, see Ref. 19). The integer number 11 was fixed for the occupation of the  $4f$  states at the Er site. An analogous approach was successfully used in the recent calculations for  $\text{RNi}_2\text{B}_2\text{C}$ .<sup>20</sup>

## III. RESULTS AND DISCUSSION

The temperature dependence of the electrical resistivity  $\rho(T)$  measured for  $\text{ErCo}_2$  in several pressures up to 8 GPa is shown in Fig. 1 (for the details in the narrow interval around  $T_C$  see Fig. 2). The ambient-pressure results are in good agreement with literature data (see, for example Refs. 21 and

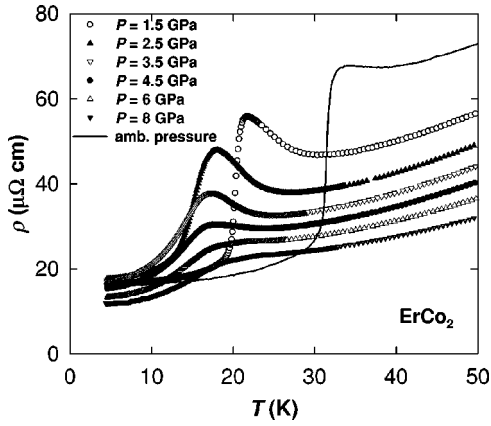


FIG. 2. Temperature dependence of electrical resistivity of  $\text{ErCo}_2$  in a narrow temperature interval around  $T_C$  at various pressures.

22). The FOMPT to magnetic ordering at  $T_C$  is accompanied by a sharp resistivity drop. Application of pressure affects considerably both the  $T_C$  value and the character of  $\rho(T)$  anomalies around  $T_C$ . The pressure-induced evolution of the resistivity below  $T_C$  has an impact on the absolute resistivity values in the paramagnetic range, nevertheless the overall shape of  $\rho(T)$  curves well above  $T_C$  is only weakly affected. As can be seen from the  $T_C$  vs  $p$  dependence in Fig. 3,  $T_C$  first decreases linearly with increasing  $p$  at a rate  $\partial T_C / \partial p = -7.9 \text{ K/GPa}$  ( $\partial \ln T_C / \partial p = 0.24 \text{ GPa}^{-1}$ ). A linear extrapolation of these data to higher pressures points to a possible critical pressure for disappearance of magnetic ordering  $p_c \approx 4.2 \text{ GPa}$ .

Measurements in pressures above 1.5 GPa, however, reveal a gradually decreasing slope of the  $T_C$  vs  $p$  dependence as long as the  $T_C$  becomes nearly pressure independent for  $p > 4 \text{ GPa}$  ( $T_C \approx 13 \text{ K}$ ). This  $T_C$  value is significantly lower than the  $T_C = 22 \text{ K}$  recently published.<sup>14</sup> Based on the following arguments we are convinced that the high-pressure  $T_C$  value determined in our experiment represents better the intrinsic behavior of  $\text{ErCo}_2$ . The rather high- $T_C$  value determined at 6 GPa in Ref. 14 is mainly due to a considerable pressure gradient in the Bridgman high-pressure cell that was mentioned already by the authors. The effect of pressure gradient in the Bridgman cell can be deduced from the comparison of the  $\rho(T)$  curves in Figs. 6(a) and (b) of Ref. 14 ob-

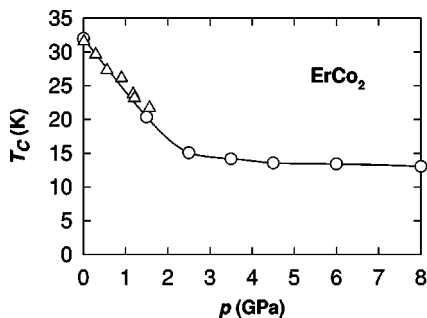


FIG. 3. The pressure dependence of  $T_C$  of  $\text{ErCo}_2$ . The triangles are the data taken from Ref. 14.

tained at a pressure of 1.58 and 1.5 GPa, respectively. Data displayed in Fig. 6(a) were measured with the sample in a liquid pressure cell that provides a hydrostatic pressure whereas the  $\rho(T)$  curve in Fig. 6(b) was obtained with the sample in the Bridgman cell. In the former case, the transition at  $T_C$  is sharp and the data just above  $T_C$  show an upturn indicating enhanced scattering of conduction electrons on spin fluctuations. In contrast, the resistivity step at the transition is considerably smeared out in data displayed in Fig. 6(b). Also, the  $T_C$  value determined in the first case is lower than in the second one (see the insert of Fig. 6). In this context we emphasize that the 1.5-GPa data displayed in detail in Fig. 2 of this paper resemble the liquid-pressure-cell data in Ref. 14 that verifies the presence of the almost hydrostatic pressure in our experiment. Moreover, the pressure-induced evolution of the  $\rho(T)$  curves in pressures beyond 1.5 GPa is much more pronounced in our results than in the Fig. 6(b) of Ref. 14. The resistivity drop at  $T_C$  becomes rapidly reduced when approaching  $p_c$  and vanishes around  $p_c$ . We consider this development as an evidence of the pressure induced suppression of IEM. This also involves the change from FOMPT at  $T_C$  to SOMPT that confirms theoretical predictions.<sup>13,23</sup>

The enhancement of resistivity in  $\text{ErCo}_2$  at temperatures just above  $T_C$ , which becomes particularly pronounced in the pressure range 1.5–3.5 GPa and vanishes above 4 GPa is ascribed to a critical conduction-electron scattering on spin fluctuations in the 3d band. Note that a formally similar development of the  $T_C$  related anomaly is observed  $\text{Er}_{1-x}\text{Y}_x\text{Co}_2$  compounds around the critical concentration  $x_c$ .<sup>14,24</sup> A closer inspection reveals, however, that this similarity reflects an intimate connection between these phenomena. Note that in both cases the value of  $H_{\text{eff}}$  becomes comparable to  $H_c$  for the metamagnetic transition. In the former case,  $H_{\text{eff}}$  is pressure invariant while  $H_c$  increases with pressure towards  $H_{\text{eff}}$ . On the other hand, in  $\text{Er}_{1-x}\text{Y}_x\text{Co}_2$  the value of  $H_{\text{eff}}$  decreases by dilution of the R sublattice towards the concentration invariant  $H_c$ . For a more detailed analysis of these phenomena we refer to the work of Hauser *et al.*<sup>14</sup>

The resistivity drop at  $T_C$  is closely connected with the stability of Co magnetism. The resistivity above  $T_C$  is mainly affected by a spin-disorder scattering on paramagnetic R moments influenced by the crystal-field interaction and by a spin-fluctuation scattering depending on the dynamics of spin fluctuations in the Co 3d band [the latter causes the above discussed  $\rho(T)$  peak just above  $T_C$ ].<sup>21,25</sup> When lowering temperature, the ferromagnetically ordered 4f moments at  $T_C$  assisted by the 5d(R)-3d(Co) hybridization produce a strong uniform exchange field acting on the Co 3d states. When this field is strong enough to split the 3d majority and minority sub-bands abruptly, the 3d-band metamagnetic state is induced by a first-order magnetic phase transition and the spin fluctuation at the Co sites are quenched. Consequently, the scattering is drastically suppressed, which yields the resistivity drop. The obvious effect of a dramatic reconstruction of Fermi surface on transport properties at the MT should be considered as well. Considering this scenario one

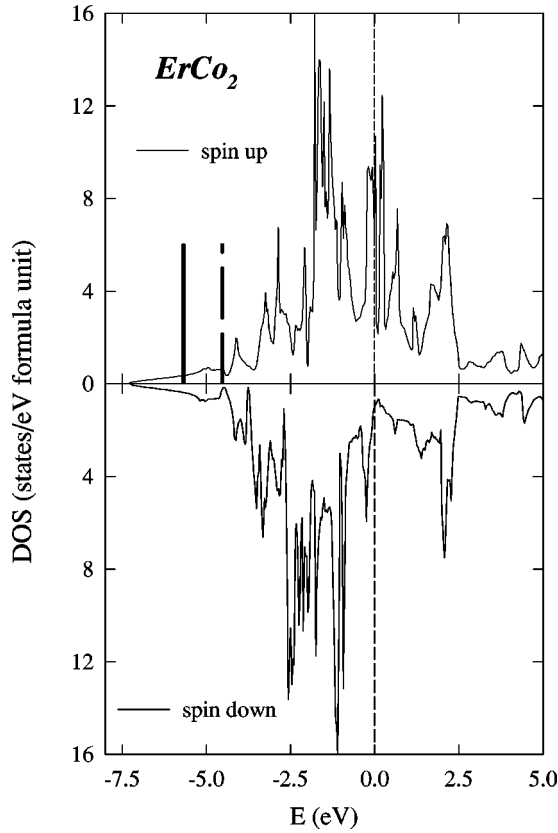


FIG. 4. The calculated total spin-polarized DOS of  $\text{ErCo}_2$  with  $a = 714.4$  pm (at ambient pressure). The Fermi energy is set to zero. The energy levels of the occupied localized  $4f_{5/2}$  and  $4f_{7/2}$  states are indicated by vertical lines (full and dashed, respectively).

may conclude that the loss of Co magnetism in  $\text{ErCo}_2$  is indicated by the vanishing resistivity drop at  $T_C$  for pressures where  $T_C$  becomes pressure invariable. For  $p > p_c$ , the pressure-induced decrease of interatomic distances of Co atoms with neighbors and a consequent increase of the overlap of  $3d$  wave functions leads to a critical broadening of the Co  $3d$  band. Consequently, the projected Co- $3d$  density of states in the vicinity of  $E_F$  decreases and the itinerant Co moment vanishes because the  $R$ -Co- $R$  exchange channel becomes ineffective to induce the IEM. Simultaneously, also the magnetic phase transition at  $T_C$  becomes second order and the pressure induced decrease of  $T_C$  ceases. The  $R$  moments then order at a “residual”  $T_C$  roughly comparable to the  $T_C$  for  $\text{ErNi}_2$  (that exhibits no  $3d$  magnetic moment because of negligible  $3d$  density of states at  $E_F$ ). The  $T_C$  value (13 K) is thus determined by the persisting conduction-electron mediated exchange interaction (Ruderman-Kittel-Kasuya-Yosida-type) coupling the localized  $R$  moments for which  $\partial T_C / \partial p$  is nearly zero.

To test this scenario we performed first-principles electronic structure calculations in the framework of DFT. The non-spin-polarized DFT calculations yield the Co-atom projected density of states (DOS) at  $E_F N_{\text{Co}}(E_F) = 1.2$  states/eV atom, which mainly originates from Co  $3d$  states [ $N_{\text{Co-}3d}(E_F) = 1.1$  states/eV atom]. From our self-consistent calculations we also deduced Stoner exchange pa-

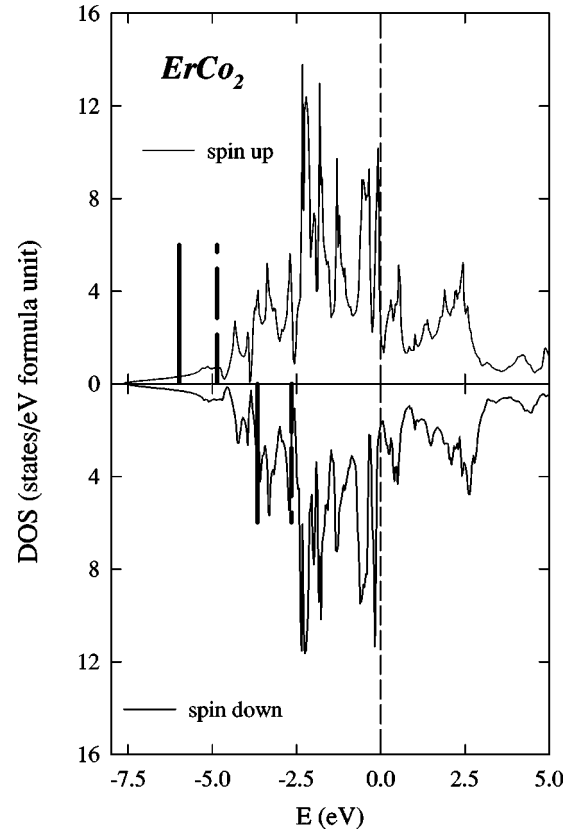


FIG. 5. The calculated total spin-polarized DOS of  $\text{ErCo}_2$  with  $a = 682.6$  pm. The Fermi energy is set to zero. The energy levels of the occupied localized  $4f_{5/2}$  and  $4f_{7/2}$  states are indicated by vertical lines (full and dashed, respectively).

rameter  $I_{\text{Co}} = 0.41$  eV. Therefore the calculated Stoner product  $I_{\text{Co}} \cdot N_{\text{Co}}(E_F)$  equals to 0.49 and does not favor the spontaneous ferromagnetic instability of itinerant Co states. In contrast the spin-polarized calculations with antiparallel alignment of the Er  $4f$  spin moments and cobalt  $3d$  spin moments converged to stable magnetic state, which has lower total energy than the non-spin-polarized state. In addition we performed a number of numerical experiments with different values of the initial exchange splitting originating from the Er  $4f$  states and Co  $3d$  states. We have found that the crucial factor driving the stability of the magnetism is the induced spin splitting of the  $R5d$  states which couples antiferromagnetically with the Co  $3d$  states. The self-consistent calculations provide the spin magnetic moments of  $M_S^{\text{Co}} = 1.13\mu_B$ ,  $M_S^{\text{Er}} = -3.25\mu_B$  inside AS and  $M_S^I = -0.19\mu_B$  in the interstitial region of the  $\text{ErCo}_2$  crystal. The corresponding DOS is shown in Fig. 4. We have found that the value of the magnetic moment of the Co  $3d$  states is significantly influenced by the shape of the sharp peaks just below the Fermi level.

In the case of  $\text{ErCo}_2$  we have also calculated the spin-polarized electronic structure for the set of ten lattice parameters smaller than the ambient-pressure value  $a_{\text{exp}} = 714.4$  pm. We have found that the  $M_S^{\text{Co}}$  is smoothly decreasing to the value of  $0.78\mu_B$  for the  $a \geq 692$  pm (which confirms the negative pressure effect on the Co moment ob-



served experimentally by magnetovolume measurements<sup>21</sup>). For values  $a \leq 688$  pm, however, the moment suddenly drops to the small value of  $M_S^{\text{Co}} < 0.1 \mu_B$ . The corresponding DOS (see Fig. 5) calculated at  $a = 682.6$  pm strongly resembles those one obtained from non-spin-polarized calculations. The main difference is connected with the larger total bandwidth as expected from comparison with Fig. 4. In the critical region  $692 > a > 688$  pm we were not able to obtain stable self-consistent solution of our DFT calculations. Considering the compressibility value for ErCo<sub>2</sub> [ $8.9 \times 10^{-3} \text{ GPa}^{-1}$  (Ref. 1)] the calculations point to the critical pressure for loss of Co metamagnetism of approximately 11 GPa. This value is nearly three times larger than the experimentally observed  $p_c$ . We are aware of the fact that our calculations cannot

involve spin fluctuations, which should play an important role in the physics of ErCo<sub>2</sub> and therefore consider the agreement between the calculated and experimentally determined critical pressure satisfactory at the present stage.

### ACKNOWLEDGMENTS

This work was supported by the Grant Agency of the Czech Republic (Grant No. 106/99/0183), Grant Agency of the Charles University (Grant No. 145/00/B FYZ), and Ministry of Education of the Czech Republic (Grant No. ME 162). One of us (O.S.) greatly appreciates the generous support from JSPS during his stay at Hiroshima University where the principal experiments were enabled.

- 
- <sup>1</sup>T. Goto, H. Aruga Katori, T. Sakakibara, H. Mitamura, K. Fukamichi, and K. Murata, *J. Appl. Phys.* **76**, 6682 (1994).  
<sup>2</sup>R. Hauser, E. Bauer, E. Gratz, M. Rotter, H. Michor, G. Hilscher, A. S. Markosyan, K. Kamishima, and T. Goto, *Phys. Rev. B* **61**, 1198 (2000).  
<sup>3</sup>E. P. Wohlfarth and P. Rhodes, *Philos. Mag.* **7**, 1817 (1963).  
<sup>4</sup>H. Yamada, *Phys. Rev. B* **47**, 11 211 (1993).  
<sup>5</sup>S. Khmelevski and P. Mohn (unpublished).  
<sup>6</sup>T. D. Cuong, L. Havela, V. Sechovsky, Z. Arnold, J. Kamarad, and N. H. Duc, *J. Alloys Compd.* **262–263**, 141 (1997).  
<sup>7</sup>D. Gignoux, D. Givord, F. Givord, W. C. Koehler, and R. M. Moon, *Phys. Rev. B* **14**, 162 (1976).  
<sup>8</sup>D. Gignoux and F. Givord, *J. Phys. F: Met. Phys.* **9**, 1409 (1979).  
<sup>9</sup>J. J. M. Franse, T. D. Hien, N. H. K. Ngan, and N. H. Duc, *J. Magn. Magn. Mater.* **39**, XX (1983).  
<sup>10</sup>Y. Berthier, D. Gignoux, and A. Tari, *J. Magn. Magn. Mater.* **58**, 275 (1986).  
<sup>11</sup>R. Hauser, E. Bauer, and E. Gratz, *Phys. Rev. B* **57**, 2904 (1998).  
<sup>12</sup>D. Bloch, D. M. Edwards, M. Shimizu, and J. Voiron, *J. Phys. F* **14**, 1217 (1976).  
<sup>13</sup>H. Yamada, *Phys. Rev. B* **47**, 11 211 (1993).  
<sup>14</sup>R. Hauser, E. Bauer, E. Gratz, M. Rotter, H. Michor, G. Hilscher, A. S. Markosyan, K. Kamishima, and T. Goto, *Phys. Rev. B* **61**, 1198 (2000).  
<sup>15</sup>N. Môri, Y. Okayama, H. Takahashi, Y. Haga, and T. Suzuki, *Jpn. J. Appl. Phys., Suppl.* **8**, 182 (1993).  
<sup>16</sup>F. Nakamura, T. Goko, J. Hori, Y. Uno, N. Kikugawa, and T. Fujita, *Phys. Rev. B* **61**, 107 (2000).  
<sup>17</sup>J. P. Perdew, S. Burke, and M. Ernzerhof, *Phys. Rev. Lett.* **77**, 3865 (1996).  
<sup>18</sup>P. Blaha, K. Schwarz, and J. Luitz, WIEN97, Vienna University of Technology, 1997 [improved and updated Unix version of the original copyrighted WIEN code by P. Blaha, K. Schwarz, P. Sorantin, and S. B. Trickey, *Comput. Phys. Commun.* **59**, 399 (1990)].  
<sup>19</sup>M. Richter, *J. Phys. D* **31**, 1017 (1998).  
<sup>20</sup>M. Diviš, K. Schwarz, P. Blaha, G. Hilscher, H. Michor, and S. Khmelevskiy, *Phys. Rev. B* **62**, 6774 (2000).  
<sup>21</sup>T. D. Cuong, L. Havela, V. Sechovsky, Z. Arnold, J. Kamarad, and N. H. Duc, *J. Alloys Compd.* **262–263**, 141 (1997).  
<sup>22</sup>E. W. Lee and F. Pourarian, *Phys. Status Solidi A* **33**, 483 (1976).  
<sup>23</sup>D. Bloch, D. M. Edwards, M. Shimizu, and J. Voiron, *J. Phys. F* **14**, 1217 (1976).  
<sup>24</sup>R. Hauser, E. Bauer, and E. Gratz, *Phys. Rev. B* **57**, 2904 (1998).  
<sup>25</sup>N. H. Duc, T. D. Hien, R. Z. Levitin, A. S. Markosyan, P. E. Brommer, and J. J. M. Franse, *Physica B* **176**, 232 (1992).